Colloids and Surfaces A: Physicochemical and Engineering Aspects 676 (2023) 132142

Contents lists available at ScienceDirect

Colloids and Surfaces A: Physicochemical and Engineering Aspects

journal homepage: www.elsevier.com/locate/colsurfa

Adsorption of surfactant molecules onto the surface of colloidal particles: Case of like-charged species

Elton L. Correia, Siddharth Thakur, Aanahita Ervin, Emma Shields, Sepideh Razavi *

School of Sustainable Chemical, Biological, and Materials Engineering, University of Oklahoma, 100 E. Boyd Street, Norman, OK 73019, USA

GRAPHICAL ABSTRACT

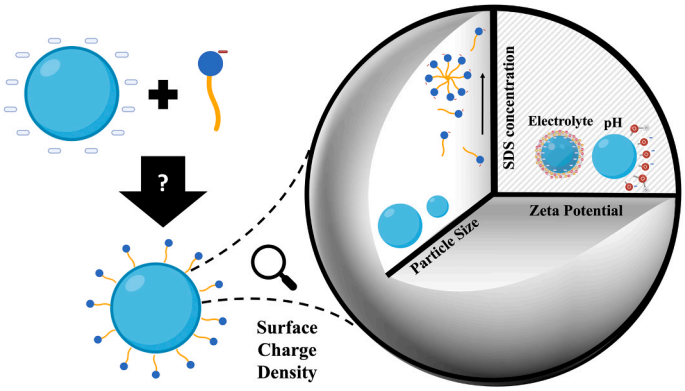

ARTICLE INFO

Keywords:
Silica nanoparticles
Sodium dodecyl sulfate
Zeta potential
Surface charge density

ABSTRACT

Mixed systems of nanoparticles and surfactants have a broad range of applications from consumer products and medicine to inkjet printing and oil recovery. The interparticle interactions can be tuned in presence of surfactants and are dependent on surface charge of both species, particle's wettability, surfactant solubility, and solution conditions such as electrolyte concentration and pH. The case of oppositely charged particles and surfactants has been extensively examined in the literature, primarily to tune the wettability of particles. In contrast, the behavior in systems of like-charged species such as negatively charged particles and anionic surfactants remains poorly understood, with conflicting findings reported in previous studies on the adsorption of surfactants. By conducting a comprehensive investigation, in this study we shed light on the factors that influence the adsorption of surfactant onto the particle surface, both promoting and preventing it, and unravel the underlying mechanisms governing such behavior. Silica nanoparticles were used as the negatively charged particle, sodium dodecyl sulfate (SDS) was used as the surfactant and potassium nitrate was used as the salt, while the pH was adjusted by potassium hydroxide and nitric acid, to investigate the effect of surfactants on the surface characteristics of the silica nanoparticles under various operating conditions. The zeta potential of particles along with the solution conductivity were obtained via mobility measurements. Using this information, the solution's Debye length and the particle's surface charge density were estimated. It was found that interpreting the outcome solely based on the zeta potential data might not reveal the adsorption of SDS onto the particle surface as no supercharging effect

* Corresponding author.
E-mail address: srazavi@ou.edu (S. Razavi).

https://doi.org/10.1016/j.colsurfa.2023.132142
Received 1 June 2023; Received in revised form 22 July 2023; Accepted 25 July 2023
Available online 27 July 2023

could be detected in some cases. However, shifting the perspective to charge density shows that SDS increased the particles charge density for pH values in the range of 2–5, corresponding to the pH conditions at which vicinal and geminal silanol groups are dissociated. This effect was more pronounced at moderate total ionic strengths between 1 and 10 mM, where SDS activity was found to be higher and the Debye length was sufficiently short. The increase in the particle's charge density was attributed to the tail-down adsorption of SDS onto the particle surface via entropically-driven interactions. These findings offer valuable insights into like-charged mixed particle/surfactant systems and bring clarity to the scientific community regarding this complex and previously inconclusive topic.

1. Introduction

Colloidal systems combining nanoparticles and surfactants have gained considerable attention in diverse sectors such as consumer care products, drug delivery, paper production, and subsurface energy recovery [1–4]. The use of surfactant/particle mixtures in these applications, with the aim of adjusting the formulation properties, is highly dependent on the interactions occurring between the species present in the system. Interactions between particles can be manipulated by altering a number of factors including the charges on both species, particles surface chemistry, and surfactants hydrophilic/lipophilic balance (HLB) [4–6]. For instance, a study by Sharma et al. showed that enhanced oil recovery (EOR) nanofluids exhibit an increased stability and effectiveness when anionic surfactants are added with the negatively-charged hydrophilic silica nanoparticles, which in turn improves recovery by altering the wettability of reservoir rocks, and reducing the interfacial tension and the oil viscosity [7]. Another example is mixed systems with application to the laundry cycle, where surfactant adsorption to particle surface has been reported to be more toxic to bacteria compared to unmodified silver nanoparticles. The study showed that negatively charged silver nanoparticles display charge reversal when mixed with oppositely charged cationic surfactants. In contrast, an increase in the magnitude of zeta potential was found in the same study when a similarly charged anionic surfactant was added to the negatively charged silver nanoparticles, which was attributed to adsorption of surfactant molecules onto the particles surface [1]. Besides from the performance standpoint in an application of interest, the nature of resulting interactions is of extreme importance from environmental remediation point of view since the nanoparticles can act as surfactant carriers to the environment [8–10]. Hence, acquiring a thorough comprehension of the interactions among species within a mixed surfactant/particle system, and the conditions that can be used to alter and tune these interactions, is crucial. This is particularly important due to their widespread application in technological advancements and the potential implications they may pose on the environment.

The interactions of oppositely charged species are well documented, especially for mixed systems including silica particles, due to their ubiquitous industrial and technological applications [4,11]. When negatively charged silica particles are mixed in solution with a cationic surfactant such as Dodecyltrimethylammonium Bromide (DTAB), the strong attractive interaction between the two species leads to the adsorption of surfactant molecules onto the surface of nanoparticles [11–13]. This phenomenon has been reported for multiple sizes of silica nanoparticles [11,12] and has been employed in tuning the particles wettability. Adsorption of cationic surfactants onto the surface of silica particles – that are hydrophilic due to the dissociation of their surface silanol groups in water – promotes the hydrophobicity of silica particles, which in turn makes the mixture of silica particles and cationic surfactant an effective stabilizer for foams and emulsions [14,15]. While at low surfactant concentrations, the attraction of the cationic surfactants polar head onto the surface of the negatively charged particle leads to an adsorbed surfactant layer, increasing the surfactant concentration can result in the formation of a bilayer on the surface of the particles, with the surfactant head groups exposed to the bulk solution [14–16]. Since the adsorption of surfactants, in form of a single layer or a bilayer, onto the surface of an oppositely charged particle can alter the particles wettability and surface charge differently, tuning the surfactant concentration is of interest in many industrial applications [13,16].

When comparing like-charged species, such as silica nanoparticles and anionic surfactants, a distinct scenario can arise in contrast to oppositely charged species. One observation is that the addition of anionic surfactant to a dispersion of silica nanoparticles can induce a more negative zeta potential in the system; this behavior has been attributed to the surfactants adsorption onto the surface of the particle, in a tail down configuration, since the polar head is repelled from the surface [17]. This type of interaction could decrease particle agglomeration and enhance the dispersion stability as the presence of anionic surfactant molecules on the particles surface leads to a pronounced repulsive interparticle interaction [17]. In contrast, it has also been reported in the literature that silica nanoparticle dispersions can be slightly destabilized by the addition of anionic surfactant, a behavior which has been attributed to an increased negative background potential that facilitates particle collisions [18]. A number of factors are reported to affect surfactant adsorption onto silica particles including the particle size, surfactant concentration, and solution properties such as its ionic strength and pH [19–22]. Even for the case of widely used anionic surfactant, sodium dodecyl sulfate (SDS), previous studies [19,20,23–29] have been inconclusive with regards to the solution conditions at which SDS adsorption onto silica particles occurs, if at all, specifically regarding the impacts salt addition and pH alterations will have on the resulting behavior, as illustrated in Fig. 1.

In presence of salt, in a mixed solution of silica nanoparticles and SDS molecules, adsorption of the surfactant onto the particle surface has been reported under certain conditions. For instance, significant adsorption has been reported at electrolyte concentrations above 10 mM and surfactant concentrations above 0.01 mM [19]. Adsorption has also been observed to increase as surfactant concentration increases under varying salt conditions until the critical micelle concentration (i.e., CMC) is reached, at which point adsorption is reported to decrease as micelles form in the solution [28]. In contrast, a complete lack of adsorption of SDS on the surface of silica particles has also been reported even in the presence of electrolyte [30]. As can be seen in Fig. 1a, with the reports available on the effects of salt addition on the adsorption, or lack thereof, in a mixed system of SDS and like-charged silica particles, it remains unclear what electrolyte conditions induce adsorption.

The effect of pH on adsorption is similarly inconclusive. At a slightly basic pH of 8, low quantities of SDS were found to adsorb onto the silica particle surface [29]. Adsorption is also reported at the more basic pH of 10 where the occurrence of adsorption was confirmed by both increased hydrodynamic size of silica particles and their supercharging [25]. In some cases, it has been suggested that SDS does not adsorb onto silica particles, specifically near neutral pH conditions [23,26,31]. In contrast, occurrence of adsorption has also been reported at a neutral pH, for SDS surfactant concentrations in the range of 3.5 mM to above CMC (~8 mM) [24,32]. A study on pH effects reported adsorption at various pH values tested (i.e., 3, 5, and 7); where a decrease in the amount of adsorbed surfactant was found upon increasing the pH, increasing the SDS surfactant concentration was reported to promote adsorption at all pH values [19]. As can be seen in Fig. 1b, while reports are available on mixed system of silica particles and SDS, the findings are inconclusive

about the pH range and surfactant concentration at which adsorption between the two species occurs. Furthermore, in mixed SDS/silica systems, without any background electrolytes, conflicting results have been reported regarding the SDS adsorption. Some authors suggest the occurrence of adsorption, while others argue its absence [27,33–35].

In order to tune the adsorption of surfactants onto the surface of similarly charged particles, it is first necessary to determine the conditions that induce adsorption. Through systematic variation of the surfactant concentration, ionic strength of the solution (i.e., by the addition of background salt and/or SDS), and the particle's surface charge, conditions needed for adsorption could be examined. For instance, pH variations affect the dissociation of the surface groups on the particles surface, altering the strength of electrostatic interactions between similarly charged species [36]. Additionally, changes in the ionic strength could affect the interactions between the surfactant molecules and the corresponding CMC value [37]. Therefore, one needs to carefully examine the impact of each contributing factor on the resulting behavior in order to specify the regions within the parametric space over which adsorption occurs between similarly charged silica particles and SDS surfactant. This work aims to shed light on a critical aspect of interfacial science, where conflicting reports have led to confusion about the factors governing the adsorption of ionic surfactants on similarly charged surfaces. The focus of the present study is to investigate the significance of factors that, in the available literature, are reported to play a role in the observed behavior in the mixed SDS/silica system and decouple the convoluted impacts of solution pH, electrolyte concentration, and surfactant concentration. From the particle mobility measurements in mixed SDS surfactant/silica particle systems, we estimate the particles surface charge density and examine the impact of different variables such as the electrolyte concentration, pH, and surfactant concentration on the adsorption behavior. Our findings provide valuable insight on the significance of these attributes with respect to adsorption behavior and highlight the range of solution properties that promote like-charge adsorption. By shedding light on the conditions that either promote or prevent adsorption, as well as the underlying mechanisms, our research contribute to the advancement of the field and brings much-needed clarity to the scientific community regarding this important yet previously inconclusive topic.

2. Materials and methods

2.1. Materials

Sodium dodecyl sulfate (SDS) was acquired from Sigma-Aldrich (purity >99 %) and purified via recrystallization according to a process reported elsewhere [5]. In short, the recrystallization procedure involves dissolving 25 g of SDS powder in 100 ml of ultrapure water, heating the solution to 30 °C while stirring with a magnetic bar until all powder is dissolved. The solution is then cooled at 5 °C overnight, followed by the vacuum filtration of precipitates and their resolubilization in 200 ml of ethyl alcohol (Fisher Scientific) via the same procedure of heating and stirring used in the first step. The solution is once again refrigerated and then vacuum filtered and rinsed with ethyl alcohol (Fisher Scientific). The final crystals are dried under vacuum afterwards. Silica nanoparticles with nominal size of 100 nm, 200 nm, and 500 nm (Fiber Optic Center Inc.), potassium nitrate (KNO_3, Fischer Scientific, purity > 95 %), nitric acid (HNO_3, Fischer Chemical), and potassium hydroxide solution (KOH, Fischer Chemical) were used as received. All the solutions and dispersions used in this study were prepared using Milli-Q® ultrapure water (18.2 MΩ·cm, Millipore, MA).

2.2. Particle dispersions

The diameter (D_{SEM}, or $2R$) of silica nanoparticles were measured via a scanning electron microscope (SEM, Thermo Quattro S field-emission). Hydrodynamic size (D_H) from dynamic light scattering (DLS) measurements and electrophoretic mobility (μ) measurements were carried out using a Nanobrook Omni (Brookhaven Instruments). Three particle sizes were employed in initial screening measurements, covering Peclet (Pe) number values in the range of 10^{-4}–10^{-1}. The Pe number informs about the ratio of diffusive to convective time scales. It is determined as per the formula: $Pe = \frac{\frac{4}{3}\pi\Delta\rho g R^4}{k_B T}$, where $\Delta\rho$ is the difference in density between the particle and the solvent, g is acceleration due to gravity, R is particle radius, k_B is the Boltzmann's constant and T is the temperature. The experiments were performed at a number of KNO_3 electrolytic concentrations (0.1, 1, 10, and 100 mM), without adding any acid or base to the dispersion. In addition, pH sweeps were performed on particle dispersions prepared at 1 mM KNO_3.

2.3. Surfactant/particle mixtures

The SDS and KNO_3 solutions were prepared separately and then mixed to achieve the final desired concentrations of SDS (i.e., 0.01, 0.1, 0.5, 1, 4, 12, 15 mM) and KNO_3 (0.01, 0.1, 1, 10, 100 mM). Thereafter, silica nanoparticles were incorporated to the mixture at a final concentration of 0.005 wt%. The mixture was sonicated for 20 min prior to any measurements. For the pH titrations, controlled amounts of HNO_3 and KOH solutions, at 1 mM and 100 mM, were added to the dispersion in order to vary the concentration of H_3O^+(H^+) and OH^- ions. For pH sweep runs in the range of 2–10, the pH of the prepared dispersion was first increased to ~10, via KOH addition, followed by its gradual

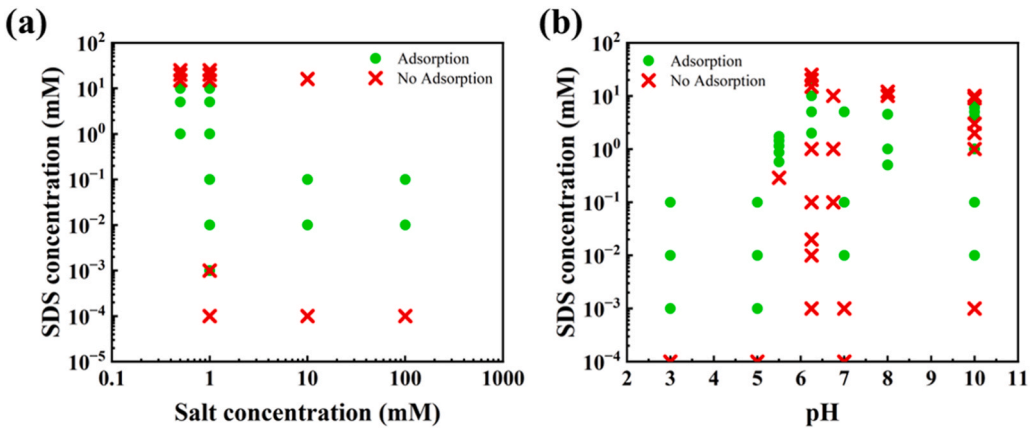

Fig. 1. Studies available in the literature on mixed SDS surfactant/silica particle systems reporting on adsorption, or lack thereof, SDS molecules onto the surface of silica particles. Available data on studies carried out at various SDS concentrations are presented as a function of (a) salt concentration, and (b) pH. Green circles (red crosses) indicate conditions at which adsorption (no adsorption) was reported. Data is reproduced from the following references [19,20,23–29].

decrease to 2 using HNO_3. SDS concentrations of 0, 4, and 12 mM were used in the pH sweep studies.

2.4. Analysis of particle zeta potential and surface charge density

The conductance values, measured and reported by the Brookhaven instrument for each sample, were utilized to determine the effective ionic concentration (c_{eff}, mol/L) as follows:

$$c_{eff} = \sum c_i = \sum \frac{\sigma_i}{\Lambda_i^0} \quad (1)$$

where σ_i is the conductance associated with the ion i, and Λ_i^0 is the molar ionic conductivity of the ion i, values of which are provided in Table 1 for the species present in the system under study. To calculate the ionic concentration of a sample, it was assumed that the molar ionic conductivities of different ions in the solution were additive [38,39]. The conductivity of the initial sample (σ_0) was taken as a reference, with its effective ionic concentration, $c_{eff\,0}$, calculated based on the molar ionic conductivity of salt ions present as follows, $c_{eff\,0} = \sigma_0/(\Lambda^0_{K+} + \Lambda^0_{NO3-})$. Then, the analysis was carried out using the conductance reading of the solution before (σ_{before}) the addition of more ions (e.g., those resulting from addition and dissociation of KOH, HNO_3, SDS), comparing it to the new conductance reading (σ_{after}), and attributing the change in the conductance value ($\Delta\sigma = \sigma_{after} - \sigma_{before}$) to the newly added ions, which in turn led to a change in the ionic strength. For instance, in a pH titration with KOH, $\Delta c = \Delta\sigma/(\Lambda^0_{K+} + \Lambda^0_{OH-})$. The resulting concentration can be calculated as $c_{eff.after} = c_{eff.before} + \Delta c$.

The calculated ionic concentration of the solution was then used in the determination of the Debye length (κ^{-1}) as follows:

$$\kappa^2 = \frac{2C_{eff}(ze)^2}{\varepsilon_0 \varepsilon k_B T} \quad (2)$$

where z is the valence of the ions and is equal to 1 in this study, e is the electron charge, ε_0 is the permittivity of vacuum, $\varepsilon$is the permittivity of water. The magnitude of κR was then calculated to determine the relative thickness of the Debye layer with regards to the particle size, with a diameter $2R$, as estimated from the SEM images (see Table 2). Thereafter, the value of κR was utilized to calculate Henry's function in each case as follows [40]:

$$f(\kappa R) = \frac{16 + 18\kappa R + 3(\kappa R)^2}{16 + 18\kappa R + 2(\kappa R)^2} \quad (3)$$

Next, the zeta potential (ζ) was calculated from the measured mobility values as follows:

$$\mu = \frac{2\varepsilon_0 \varepsilon \zeta}{3\eta} f(\kappa R) \quad (4)$$

where μ is the mobility [(μ/s)/(V/cm)] and η is the viscosity of water (Pa.s). Thereafter, the particle surface charge density (ρ_s, μC/cm^2) was determined from the Gouy-Chapman formulation that relates the surface charge density to the zeta potential (ζ), assuming that the zeta potential is equal to the Stern potential, as follows [41]:

Table 1
Molar ionic conductivity (Λ_i^0) of the ions present in the system under study [39,45].

Ion	Λ_i^θ (cm^2.s/mol)
H^+	349
OH^-	198
K^+	73.5
NO_{3-}	71.5
DS^-	23.4
Na^+	50.1

Table 2
Properties of silica nanoparticles used in this study: particle diameter estimated from SEM analysis (D_{SEM}), hydrodynamic diameter (D_H) obtained from the DLS measurements carried out in 0.1 mM background KNO_3 electrolyte solution, value of particle's zeta potential (ζ) measured at the same conditions, and the charge densities estimated using κR determined based on the measured D_{SEM}. The pH for all dispersions was 5.4 ± 0.2.

Silica particle nominal size (nm)	D_{SEM} (nm)	D_H (nm)	ζ (mV)	ρ_s (μC/cm^2)
100	100 ± 30	129 ± 1	–57 ± 1	0.29 ± 0.01
200	210 ± 40	253 ± 4	–58 ± 6	0.26 ± 0.03
500	500 ± 60	529 ± 7	–72 ± 2	0.31 ± 0.02

$$\rho_s = \frac{2\varepsilon_0 \varepsilon k_B T \kappa}{e} \sinh\left(\frac{e\zeta}{2k_B T}\right) \quad (5)$$

where the zeta potential (ζ) was estimated based on the measured particle mobility (μ) from Eq. 4. This equation was used to avoid arbitrary assumptions on the thickness of the slip plane [42–44]. It is important to note that to determine the surface potential (and the corresponding surface charge density) experimentally, titrating the particle dispersion with a known amount of ions is required [42].

2.5. Model for the particle zeta potential at various pH values

It is possible to relate the zeta potential to the charged groups at the surface at various pH values based on the following implicit equation derived from the Gouy-Chapman formulation [41]:

$$\frac{-eN_A}{1 + 10^{(pKa-pH)} \exp\left(-\frac{e\zeta}{k_B T}\right)} = \frac{2\varepsilon_0 \varepsilon k_B T \kappa}{e} \sinh\left(\frac{e\zeta}{2k_B T}\right) \quad (6)$$

where N_A is the number density of acid sites, which is determined based on the estimated surface charge density (ρ_s), and pKa is the acid strength. The provided equation assumes that only acid groups are present on the surface. In order to determine the appropriate value for the number charge density, the region where the zeta potential remains nearly constant with pH alterations, (in the current study pH range of 5–7), was taken as a reference. Right and left sides of the equation were solved independently, and their difference was minimized by varying the guessed value for ζ.

3. Results and discussion

3.1. Characterization of particle dispersions

Results of SEM imaging of particles and the characterization of particle dispersions at low background salt concentration of 0.1 mM KNO_3 are provided in Table 2. The pH value, averaged over all the dispersions used in these studies, was 5.4 ± 0.2. It should be noted that silica particles of size larger than 500 nm, for which $Pe \geq 1$, were not deemed suitable for this study as particle sedimentation impacts the DLS measurements.

3.1.1. Effect of electrolyte

Variation in the electrolyte concentration was carried out in particle dispersions of different sizes in order to examine the severity of the resulting aggregation. Initial experiments were carried out in the absence of SDS to determine the salt concentrations that can be used in the study of mixed surfactant/particle systems to generate reliable data from the DLS measurements. The effect of salt concentration on the measured hydrodynamic diameter (D_H) of the particles is presented in Fig. 2a and the corresponding autocorrelation function for these samples are provided in the Supporting Information. As expected, with

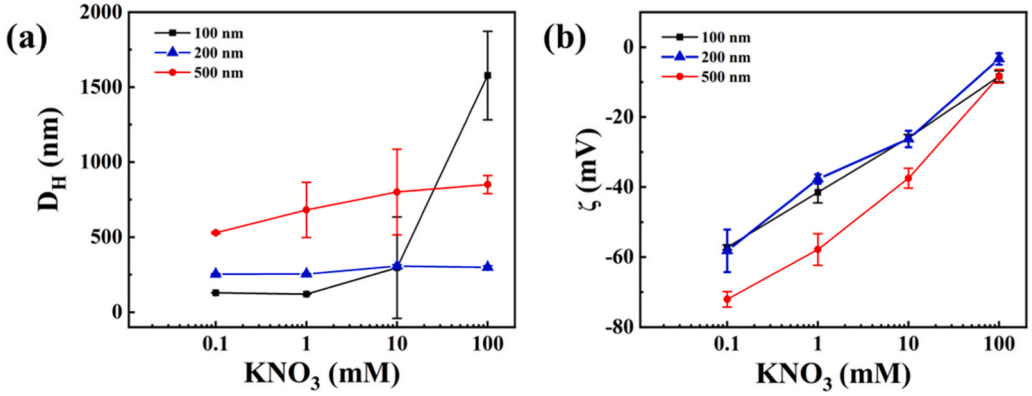

Fig. 2. Effect of KNO_3 electrolyte concentration on (a) hydrodynamic size (D_H) and (b) zeta potential of particle dispersions with particles of size 100 nm (black square), 200 nm (blue triangle), and 500 nm (red circle).

increasing the salt concentration, the average particle size also increased. As the salt concentration increased in the range of 1–100 mM, the rate of increase in the measured hydrodynamic size was larger for the 500 nm particle sample, which could be interpreted as aggregate formation even at low salt concentrations (1 mM) in this case and faster sedimentation for aggregates forming by the larger 500 nm particles. As the salt loading was further increased to 100 mM KNO_3, the 100 nm particles formed aggregates of larger size (1578 ± 296 nm) compared to those resulted from 200 nm (298 ± 10 nm) and 500 nm particles (850 ± 61 nm), which can be explained by two factors as follows. Firstly, the reduced zeta potential at the high salt concertation promotes aggregation; secondly, there is a higher likelihood of particle collision in the case of 100 nm particles, which could also promote aggregation. The latter is due to the higher number density of 100 nm particles compared to 200 nm particles for dispersions prepared at the same particle concentrations by weight used in these DLS studies; i.e., there are 8 silica particles of 100 nm size for every particle of 200 nm size, in dispersions prepared at the same concentration by weight. Additionally, based on Stokes-Einstein equation for Brownian motion, the diffusion constant of colloidal particles is inversely proportional to their size. Since the diffusion coefficient of 100 nm particles is twice as large as the value for 200 nm particles, the probability of particle collisions is further enhanced in the former sample.

Fig. 2b depicts the variation in the measured zeta potential of the particle dispersions as a function of electrolyte concentration. It can be observed that zeta potential exhibited a logarithmic dependence on the ionic strength, where increasing the electrolyte concentration led to a reduced magnitude of the zeta potential. Moreover, with increasing the electrolyte concentration, the magnitude of zeta potential reduced for all particle dispersions. This trend is expected due to screening of particle surface charges by increasing the ionic strength in the bulk, which results in a shorter Debye length. The value of κ^{-1} estimated from the calculated effective concentrations reduced from 17.8 ± 0.7 nm at 0.1 mM KNO_3 to 1.0 ± 0.1 nm at 100 mM KNO_3.

It is important to highlight that the hydrodynamic size measurements could be used as an indication for colloidal stability vs. aggregate formation. Therefore, these experiments were run as screening tests in order to determine whether such effects (e.g., aggregation) are present in particle dispersions, at various solution conditions of interest, because they could impact the results and interpretation of the mobility measurements, which are then used to infer about SDS adsorption. Since the 500 nm particle samples exhibited an increase in measured particle size at all electrolyte concentrations, we limited the study of mixed surfactant/particle systems to the 100 nm and 200 nm particle sizes only. In the latter two cases, we also restricted the interpretation of the data obtained via hydrodynamic size measurements to electrolyte concentration below 10 mM in order to avoid aggregation effects impacting the results of the measurements. By focusing solely on 100 nm and 200 nm particles, the range of Peclet numbers (*Pe*) investigated fell between 1×10^{-4}–2×10^{-2}, ensuring that the measurements remained unaffected by gravity.

3.1.2. Effect of pH

In order to examine the response of particle-only dispersions to alterations in pH and the differences between the characteristics of the two particle sizes under study (i.e., 100 nm vs. 200 nm), zeta potential measurements were carried out at different pH values (at 1 mM KNO_3) results of which are displayed in Fig. 3. It is worth noting that no pronounced aggregation was observed for the systems analyzed here. For the case of 100 nm particle dispersions (Fig. 3a), at a neutral to high pH range (6−9), the value of measured zeta potential remained nearly constant with pH alterations. This behavior could be attributed to the complete dissociation of the surface silanol groups present on the silica particles, which may possess several pKa values depending on their characteristics [46–48]. At low pH values (pH <5), due to the presence of excess hydronium (H_3O^+) ions in the bulk, there was a reduced tendency for ionization of the surface silanol groups, which consequently resulted in a decrease in the magnitude of the measured zeta potential. By applying the model described in Eq. 6, the pKa value associated with the best fit was found to be ~2.1, which is aligned with the pKa value attributed to vicinal silanol groups [48].

For the 200 nm dispersion (Fig. 3b), a similar response to pH alterations was captured. Modeling the zeta potential values obtained from the pH sweep in case of 200 nm particle dispersions yielded a pKa value of ~2.9, which agrees with the pKa values for external geminal silanol groups [48]. This corroborates the higher surface charge density found for 100 nm particles when compared to the 200 nm (Table 2), since vicinal groups are associated with silanol that are in proximity to each other. In addition, at the high pH region, there was a further increase in the magnitude of the zeta potential, which might be associated with isolated silanol groups (pKa ~8.9) present in the 200 nm particle surface [47,48]. To incorporate this factor when fitting the data with the model, the left-hand side of the Eq. 6 was calculated with both pKa values (2.9 and 8.9) and summed.

3.2. Characterization of mixed surfactant/particle systems

3.2.1. Effect of SDS at various pH

The behavior of the mixed surfactant/particle system was analyzed as a function of the solution pH, for the salt (KNO_3) concertation of 1 mM. It should be noted that for the mixed surfactant/particle systems, no pronounced increase in the measured particle size was observed as the pH was lowered. Fig. 4**a** illustrates the change in the measured zeta potential for mixtures prepared with 100 nm particle dispersions. The presence of surfactant affects the particle surface characteristics, as

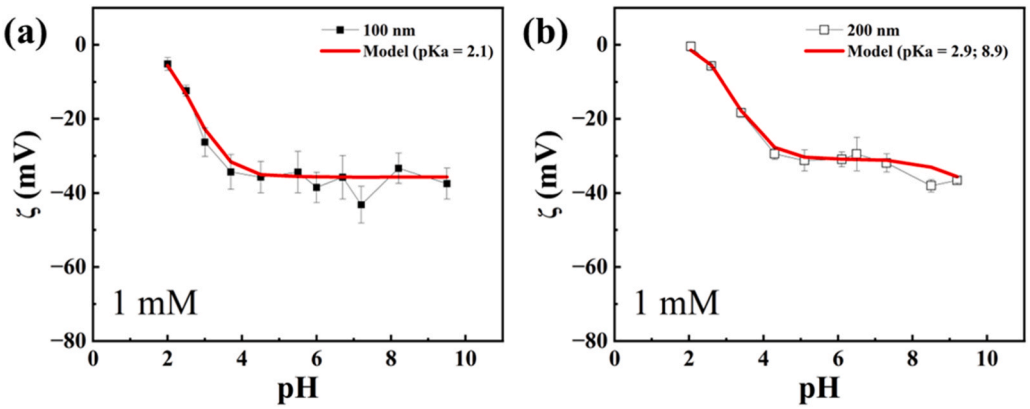

Fig. 3. Effect of pH on the zeta potential of (a) 100 nm (b) 200 nm particles. The model was calculated based on Eq. 6 and a pKa input value of 2.1 was used to fit the zeta potential data obtained for 100 nm particles, while a combination of pKa values of 2.9 and 8.9 were used for the case of 200 nm particles.

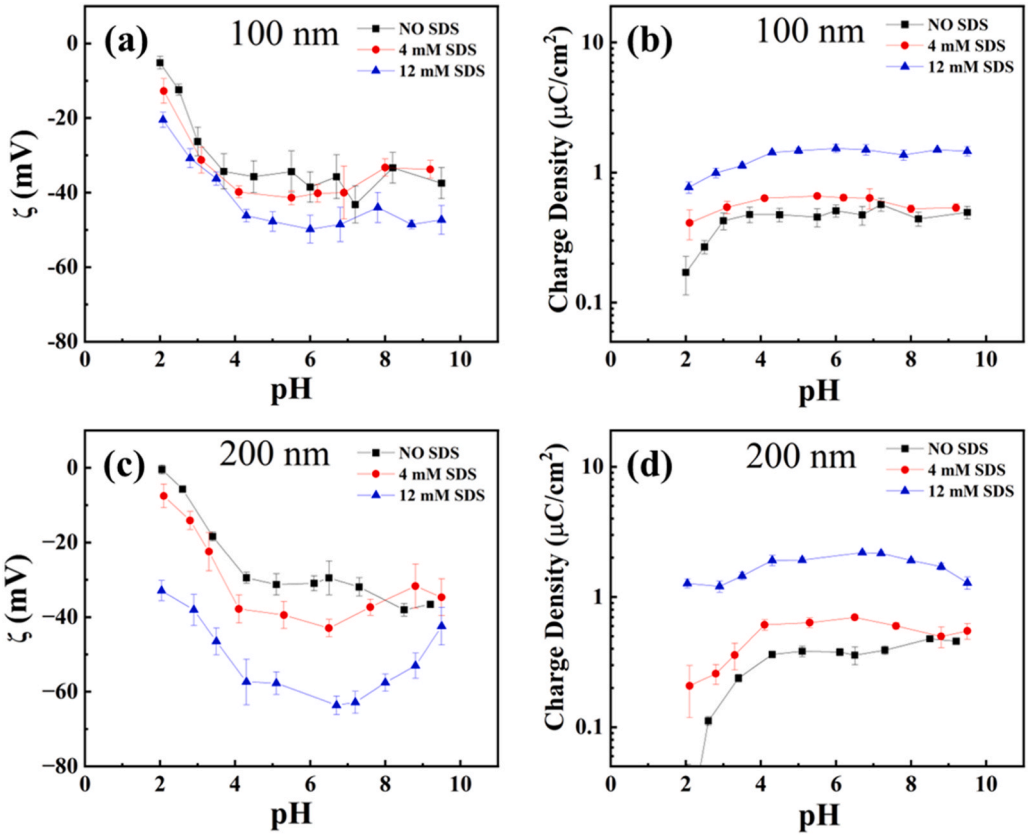

Fig. 4. Effect of surfactant concentration on (a, c) zeta potential, and (b, d) surface charge density of 100 nm and 200 nm silica particle dispersions measured as a function of solution pH at salt concentration of 1 mM.

manifested in the increased zeta potential magnitude across pH values smaller than 5. Measuring a more negative zeta potential value, in presence of the surfactant within the mixture, can be attributed to the adsorption of surfactant molecules onto the particles surface. At a neutral to high pH range (6–9), the effect of surfactant addition on the zeta potential was less pronounced compared to its impact at low pH range (2–5). This trend is expected since at the high pH range, there is a higher extent of dissociation for the silanol groups present on the particle surface, which may have curtailed the interaction between the silica particle surface and surfactants due to charge-charge repulsion. With regards to the determination of electrophoretic mobility in mixed particle/surfactant systems under study, it is worth noting that the scattering that results from the free unadsorbed surfactant molecules is considered negligible because the scattering intensity is proportional to the volume of the scattering object.

Fig. 4b presents the calculated charge density on the particle surface, for the case of 100 nm particles, and its variation as a function of pH and SDS concentration. It is noteworthy that the charge density on the silica surface remained higher for all cases involving SDS, at all pH ranges under study, compared to the values calculated for the particle-only dispersions in the absence of SDS. In addition, the particle's surface charge density was higher in samples containing 12 mM SDS compared to those prepared at 4 mM SDS. This result contradicts another study mentioned beforehand, where SDS adsorption was found to decrease at concentrations higher than CMC (~8 mM for SDS at these salt conditions) [28]. However, as stated elsewhere, surfactant adsorption reaches

a plateau when its concentration in the bulk has reached the CMC value (i.e., the total concentration of surfactant in the bulk plus the adsorbed state is much higher than the CMC), in which case additional surfactant molecules are responsible for populating the micelles [49], which is in line with our findings that the maximum adsorption is at concentrations above the CMC. Therefore, the higher magnitude of zeta potential observed for cases involving SDS, can be attributed to the presence of charged species on the silica particle surface.

The adsorption of surfactant molecules onto the surface of silica particles, in a tail-down configuration, can be attributed to entropically-driven interactions; the hydrophobic tails of the surfactant molecules, when dispersed in the solution, require numerous ordered water molecules for their solvation. However, when the surfactant tails are adsorbed onto a surface, the water molecules are free to interact with other molecules and assume other configurations, increasing the entropy of the system [50,51]. Such adsorption of ionic surfactants onto the surface of like-charged particles has been attributed to hydrophobic interactions despite the electrostatic repulsion of the species [1,52].

Fig. 4**c** illustrates the change in zeta potential at various SDS concentrations for 200 nm particles. When comparing the particle-only to SDS/silica mixtures, there is a clear increase in the magnitude of the zeta potential when SDS is present for almost all pH values. Interestingly, at the higher pH values (pH $\geq$ 8) there is a decrease in the magnitude of the zeta potential for both samples containing SDS, whilst the particle-only dispersion showed an increase in the magnitude of the zeta potential, as discussed previously. This corroborates the earlier finding that isolated silanol groups (pKa $\sim$ 8.9) are present in the 200 nm particles. While the dissociation of these isolated silanol groups, at high levels of pH, generates an increase in the charge density for the particle-only systems, it deters SDS adsorption and therefore leads to a decrease in the particle surface charge density for the samples with SDS (Fig. 4d). Therefore, adsorption of SDS is considered to be at its maximum at lower and intermediary pH values, in the range of 5–8, and decreases upon increasing the pH to highly basic conditions (pH $\geq$ 8).

3.2.2. *Effect of SDS at various electrolyte concentration*

In order to isolate the effect of added electrolyte on the overall ionic strength of the solution and the resulting impact on the surfactant/particle interactions, variation in the salt and surfactant concentration was carried out at a fixed solution pH. This was done by considering not only the background salt concentration but also the effect of any added electrolyte to the overall ionic strength (i.e., $I = I_{KNO_3} + I_{KOH} + I_{HNO_3} + I_{SDS}$) of the mixture. Fig. 5a depicts the measured change in the zeta potential resulting from varying the overall ionic strength in the solution at pH values between 5 and 6. As expected, for the particle-only dispersions (i.e., no SDS systems), a decrease in the magnitude of the measured zeta potential was observed with an increase in the ionic strength [53]. This trend is expected and is attributed to the screening of particle surface charges by the ionic cloud and the compression of the electrical double layer [54,55].

In the presence of surfactants, however, a deviation from this trend was observed depending on the SDS concentration. At low surfactant concentrations ($c_{SDS} \leq 0.01$ mM), the trend was similar to that observed for no SDS systems. For intermediate SDS concentrations ($0.1 \leq c_{SDS} \leq 0.5$ mM), results of some measurements showed deviations from the trend observed for the no SDS condition. Furthermore, as the surfactant loading was increased ($c_{SDS} \geq$ 1 mM), the zeta potential became more negative, which could be caused by the presence of surfactants on the particle surface, where the excess negative charges could be attributed to the added SDS head groups.

This was further evidenced when comparing charge densities, depicted in Fig. 5b. For a particle-only system, the surface charge density increases as the ionic strength of the system is increased [55]. This results from the assumptions made relating the charge density to the zeta potential (Eq. 5), i.e., that the zeta potential is equal to the Stern potential. At low ionic strength conditions, the electric double layer is larger, with fewer ions populating it. In contrast, at higher concentration of electrolytes, there is an increase in the number of ions populating the double layer surrounding the particle system, which is associated with a higher charge density [56]. It should be recognized that at high ionic strengths (i.e., 100 mM), significant deviations can occur between the zeta potential and the Stern potential [57]; therefore, results obtained under these conditions should be interpreted with caution especially considering particle aggregation that may occur at such high ionic concentrations (see discussion on Fig. 2a).

For the mixed systems, at low ionic concentrations, the density of surface charges on the particle was lower and closer to the estimated values for the particle-only systems. At high ionic concentrations in mixed surfactant/particle systems, presence of surfactant molecules enhanced the magnitude of the particle surface charge density. However, the difference between the charge density of the mixed system in comparison to the particle-only system is maximized at moderate ionic strengths (1 and 10 mM). Thus, there is a tradeoff for increasing the overall ionic strength, which changes both the Debye length and the measured zeta potential. This is expected since the activity of ionic surfactants are known to be affected by the electrolyte concentration in the system. For instance, the bulk concentration of SDS required to achieve a certain surface adsorption concentration on the air-water interface decreases by two orders of magnitude when comparing systems at 0 and 100 mM NaCl [58].

From the perspective of entropic interactions, higher ionic strengths are associated with a lower water activity [59]. Each surfactant tail requires a number of water molecules structured around it for the purpose of solvation. By increasing the ionic strength of the solution, water molecules also solvate the ions, which, in turn, decreases the total number of molecules available to solvate the surfactant tails [50].

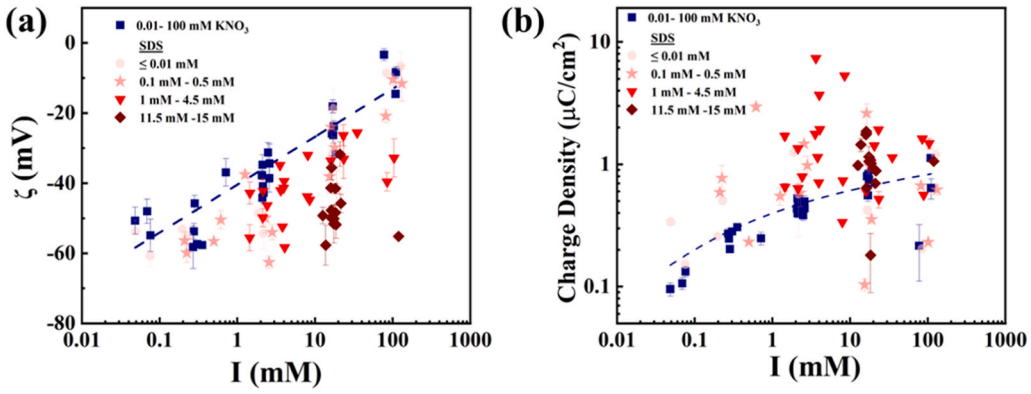

Fig. 5. Effect of variation in the added salt (KNO_3) and surfactant (SDS) concentration, reflected in an increase in the total ionic concentration (I) of the dispersion, on (a) zeta potential and (b) charge density of the particles. Data includes measurement on both 100 nm and 200 nm particle samples with pH values in the range of 5–6. Data belonging to particle-only dispersions, prepared at different KNO_3 concentrations, are shown using blue symbols, whereas measurements obtained for mixed SDS/silica samples, obtained at different KNO_3 and SDS concentrations are shown using red symbols. Darker tones of red represent higher SDS concentrations.

Moreover, the increase in the ionic concentration of solution screens the electric field that causes the repulsion between the charged particle surface and the surfactant head. Both these factors contribute to the promotion of surfactant adsorption onto the surface of like-charged particle in presence of higher salt concentrations in the solution [50]. Therefore, there are signs of adsorption at moderate pH conditions (in the range of 5–6). Nevertheless, since both SDS and KNO_3 can impact the ionic strength of the solution, we have taken the data analysis one step further to deconvolute the surfactant and salt contributions, as discussed in the next section.

3.2.3. *Effect of SDS from the perspective of mean ionic product*

To decouple the effects of SDS on the ionic strength of the solution, from that of the added KNO_3 salt, and examine the origin of the observed supercharging on the particle surface, we used the mean ionic product (c^*), which accounts for the impact of ions, other than those resulting from SDS, present in the system to normalize the concentration of surfactant solutions at various background salt concentrations. In this approach, the mean ionic product is defined as follows [60]:

$$c^* = \gamma_{\pm}(c_{SDS+other\ \ ions} \times c_{SDS})^{1/2} \tag{6}$$

where c_{SDS} is the concentration of SDS, $c_{SDS+other\ ions}$ is the concentration of all species, $\gamma_{\pm}$ is the average activity coefficient of the system, calculated from the Debye-Hückel equation as follows:

$$\log\gamma_{\pm} = -\frac{0.5115 \times \sqrt{I}}{1 + 1.316 \times \sqrt{I}} + 0.055 \times I \tag{7}$$

Using the mean ionic product to analyze the measured data allows for the comparison of the results in mixed SDS/silica systems to those obtained from particle-only dispersions with a similar ionic strength. Data on the particle's zeta potential and surface charge density as a function of the effective ionic concentration (c^*), for samples containing SDS, is shown in Fig. 6. For comparison, the corresponding values for samples without SDS, i.e., particle-only dispersions, are also provided in the figure as a function of the total ionic strength (I). In addition, data available in the literature on the mixed SDS/silica system, obtained from various references [24,25,28,29,34], are also displayed on the same plot. It is worth noting that inferring about the SDS adsorption, or lack thereof, onto the particle surface, solely based on the zeta potential results shown in Fig. 6a, is not trivial since there are multiple factors at play in case of mixed systems. There is a large scatter in the data, both from this work and those reported elsewhere [24,25,28,29,34]. To illustrate the clear distinction between the data obtained for mixed surfactant/particle systems with SDS (full symbols) and those for particle-only dispersions without SDS (open symbols), the particle surface charge density was calculated from the measured zeta potential in each case, as shown in Fig. 6b. As can be seen, at the same effective ionic concentration, particle dispersions containing SDS exhibit a higher charge density when compared to a sample without SDS. This effect appears to be enhanced at larger SDS concentrations, which is expected since there is a higher activity of SDS molecules in the bulk. It is important to note that some of the data taken from the literature pertain to particles that are not spherical in shape (fumed silica). For those cases, the reported D_H was used in the charge density calculations and therefore the results exhibit greater variability. Compared to Fig. 1a where a definitive region indicating SDS adsorption was not clearly delineated, Fig. 6b offers a more distinct differentiation between the characteristics of samples with SDS and those of particle-only dispersions.

3.2.4. *Effect of SDS at various pH and electrolyte concentration*

To determine the extent of SDS adsorption onto the silica particle surface for a mixed system that is not at neutral pH, an analogous analysis to the one conducted in the previous section was performed on data acquired at various pH values. The data was generated at two pH ranges that were considered "low" (i.e., pH$\leq$ 5) and "high" (i.e., pH $\geq$ 6). These values were selected based on the response of the particle-only dispersions to pH alterations, where at low pH range, reducing the pH resulted in a decrease in the magnitude of the zeta potential, and over the high pH range, increasing the solution pH did not have a pronounced impact on the measured zeta potential, as depicted in Fig. 3.

Fig. 7 illustrates the measured zeta potential and calculated charge density corresponding to measurements carried out at low and high pH ranges for SDS/silica mixtures using data from both 100 nm and 200 nm systems. Fig. 7a shows that the measured values of zeta potential in the mixed surfactant/particle samples have a higher magnitude compared to those obtained for the particle-only dispersions in presence of KNO_3. The same trend is observed in Fig. 7c, where the charge density for samples containing SDS is overall higher than those without SDS. It is worth noting that the results at low pH show a more pronounced difference when comparing the particle surface charge density for samples containing surfactant with those of dispersions without SDS. This can be explained by the fact that at these lower pH values, the system is closer to the isoelectric point of silica particles (see Fig. 3), indicating a lower density of surface charges on the particle, which could promote the SDS adsorption onto the particle surface. It is important to note that the variation in ionic strengths for particle-only systems are not only due to different KNO_3 concentrations but also acid addition. Therefore, there is a downward trend of surface charge density with ionic strength as the acid concentration is higher. Such downward trend is not present in

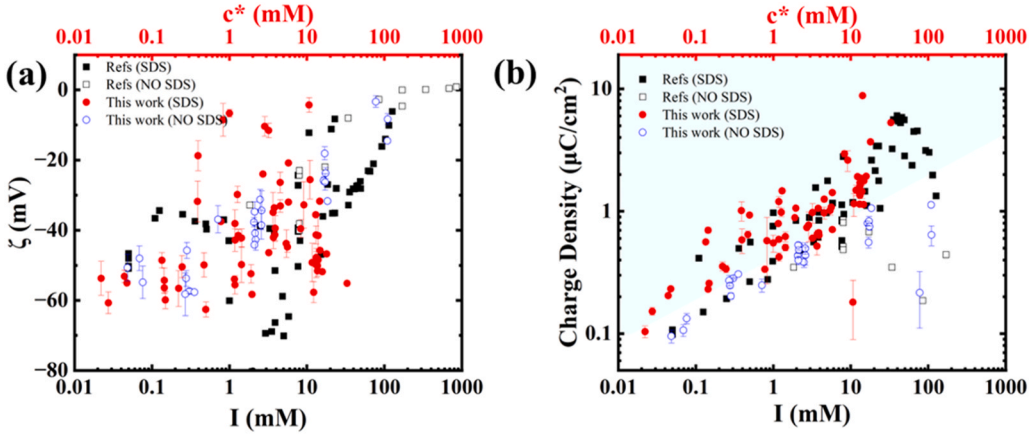

Fig. 6. Effect of variation in the salt and surfactant concentration, at pH values between 5 and 6, in 100 nm and 200 nm particle dispersions: (a) zeta potential and (b) surface charge density. Data is plotted as a function of the ionic strength (I) for samples without SDS and mean ionic product (c^*) for samples with SDS. Our data is shown along with data taken from several references [24,25,28,29,34]. Full symbols correspond to mixed surfactant/particle samples and open symbols belong to particle-only dispersions (black squares for reference data, red and blue circles for data from this work). Area shaded in teal colour corresponds to data for mixed surfactant/particle systems falling in the region for which the resulting particle surface charge density is higher than that obtained for salt only particle dispersions (no SDS), which is attributed to the adsorption of SDS onto the particle surface in the former case.

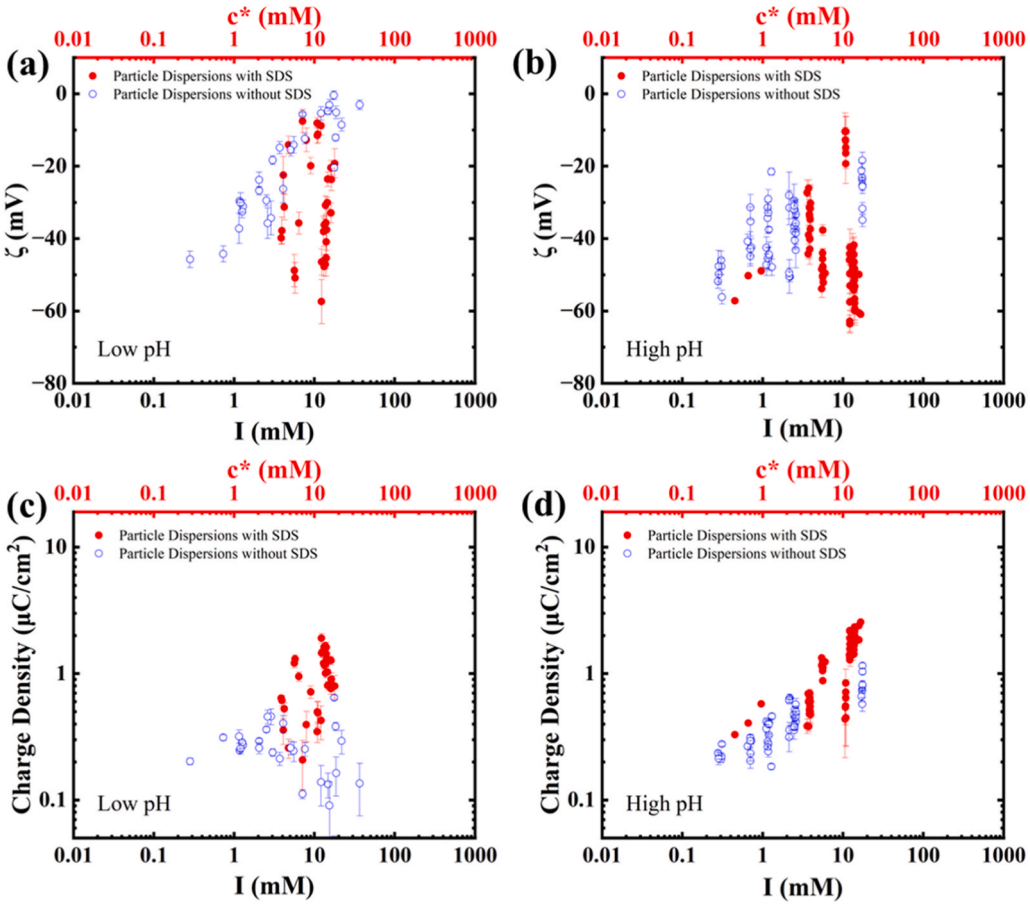

Fig. 7. Effect of variation in the salt and surfactant concentration at fixed pH on (a, b) zeta potential, (c, d) charge density, as a function of total ionic concentration (I) for samples without SDS, and effective concentration (c^*) for samples with SDS. Top charts (a, c) show data obtained at "low pH" values (pH $\leq$ 5), while the bottom charts belong to those measured at "high pH" range (pH $\geq$ 6). Data obtained from both 100 nm and 200 nm particle samples were used in generating these plots.

systems with SDS even though the particles were exposed to the same pH conditions.

Fig. 7b presents systems at high pH range, which do not exhibit a clear distinction depending upon the presence of SDS. This is also evidenced in Fig. 7d where the calculated charge density for some of the mixed surfactant/particle samples falls in the region that belongs to particle-only data in presence of KNO_3 salt, even at high effective concentrations of SDS. Higher pH values are associated with a higher surface charge on the silica surface, as shown in Fig. 4b and d, which may hinder adsorption. Nevertheless, at high pH and high SDS concentration, there is indeed an elevated charge density observed, suggesting that even under these conditions, some level of adsorption occurs.

4. Conclusions

In this work, we performed a comprehensive study on mixed systems of silica particle and SDS surfactant. We examined changes in particle surface properties in response to alterations in solution pH and electrolyte concentration in order to shed light on factors that promote or prevent surfactant adsorption onto the particle surface in case of like-charged SDS/silica system. We applied dynamic light scattering to measure the particles hydrodynamic diameter, electrophoretic mobility measurements to probe the zeta potential under various dispersion conditions, and estimated the surface charge density from the obtained conductivity and mobility values. We decoupled the contribution of SDS to the ionic strength of the solution and alteration of zeta potential for negatively charged silica nanoparticles. These studies aided in identifying variable domains in which SDS adsorption onto silica particles is more or less likely to occur, and the conditions at which it may affect the zeta potential readings, which are usually used as a direct indication of surfactant adsorption. We showed that charge density is a more fit parameter for identifying adsorption of SDS onto silica particles. Our findings reveal that SDS adsorption onto the silica surface can occur, through entropically-driven interactions, under certain conditions as follows.

1. At moderate pH conditions (between 5 and 6), SDS adsorption takes place over the range of the ionic strengths studied in this work (0.1–100 mM). However, it might not decrease the particles zeta potential (i.e., supercharging of the particle surface may not be detected);
2. An acidic environment improves surfactant adsorption and "supercharging" effect;
3. Basic environments could hinder adsorption and supercharging in the presence of isolated silanol groups on the silica surface; however, high SDS concentrations ($c^* \geq$ 10 mM) might overcome the pH effect.
4. There is a tradeoff between the ionic strength decreasing the particle's zeta potential and dispersion's Debye length, which leads to a maximum of increase in the magnitude of charge density caused by surfactants adsorption on the surface of particles to take place in the range of 1–10 mM of total ionic strength.
5. The supercharging effect is less pronounced if the particle's zeta potential is high (–60 mV) prior to the addition of the SDS surfactant and becomes more pronounced as the zeta potential is reduced,

which can be achieved by increasing the ionic strength of the solution.

The fundamental understanding obtained in this work on the mixed system of like-charged species, utilizing SDS/silica as a model system, and the insights offered on the impact of solution properties such as pH and electrolyte concentration on the surfactant adsorption, represents a significant advancement in the field. The framework provided by this research serves as a valuable guide for comprehending the behavior in other like-charged mixed systems. Beyond its immediate implications, these findings have far-reaching impacts in the field, considering the extensive technological applications and environmental significance of mixed systems involving similarly charged particles and surfactants.

CRediT authorship contribution statement

Elton Correia: Data curation, Formal analysis, Visualization, Writing – original draft, Validation, Writing – review & editing. **Aanahita Ervin:** Data curation, Formal analysis, Visualization, Writing – review & editing. **Emma Shields:** Data curation, Formal analysis, Visualization, Writing – review & editing. **Siddharth Thakur:** Data curation, Formal analysis, Visualization, Writing – review & editing. **Sepideh Razavi:** Methodology, Investigation, Validation, Writing – review & editing, Supervision, Project administration, Resources, Funding acquisition.

Declaration of Competing Interest

The authors declare no known competing financial interests or personal relationships that could have influenced the work reported in this paper.

Data Availability

Data will be made available on request.

Acknowledgments

The authors acknowledge the support from the US National Science Foundation (NSF) through the awards NSF CBET-1934513 and NSF CAREER CBET-2144020 for providing funding for this project.

Appendix A. Supporting information

Supplementary data associated with this article can be found in the online version at doi:10.1016/j.colsurfa.2023.132142.

References

[1] J. Hedberg, et al., Interactions between surfactants and silver nanoparticles of varying charge, J. Colloid Interface Sci. 369 (1) (2012) 193–201.
[2] K. Landfester, L.P. Ramirez, Encapsulated magnetite particles for biomedical application, J. Phys.: Condens. Matter 15 (15) (2003) S1345.
[3] A. Barhoum, et al., Effect of cationic and anionic surfactants on the application of calcium carbonate nanoparticles in paper coating, ACS Appl. Mater. Interfaces 6 (4) (2014) 2734–2744.
[4] M. Almahfood, B. Bai, The synergistic effects of nanoparticle-surfactant nanofluids in EOR applications, J. Pet. Sci. Eng. 171 (2018) 196–210.
[5] E.L. Correia, et al., Contamination in sodium dodecyl sulfate solutions: insights from the measurements of surface tension and surface rheology, Langmuir 38 (23) (2022) 7179–7189.
[6] B.J. Lele, R.D. Tilton, Colloidal depletion and structural force synergism or antagonism in solutions of mutually repelling polyelectrolytes and ionic surfactants, Langmuir 35 (48) (2019) 15937–15947.
[7] T. Sharma, S. Iglauer, J.S. Sangwai, Silica nanofluids in an oilfield polymer polyacrylamide: interfacial properties, wettability alteration, and applications for chemical enhanced oil recovery, Ind. Eng. Chem. Res. 55 (48) (2016) 12387–12397.
[8] E.-J. Bae, et al., Effect of chemical stabilizers in silver nanoparticle suspensions on nanotoxicity, Bull. Korean Chem. Soc. 32 (2) (2011) 613–619.
[9] Y. Ju-Nam, J.R. Lead, Manufactured nanoparticles: an overview of their chemistry, interactions and potential environmental implications, Sci. Total Environ. 400 (1–3) (2008) 396–414.
[10] E. Nourafkan, Z. Hu, D. Wen, Nanoparticle-enabled delivery of surfactants in porous media, J. Colloid Interface Sci. 519 (2018) 44–57.
[11] S.B. Velegol, et al., Counterion effects on hexadecyltrimethylammonium surfactant adsorption and self-assembly on silica, Langmuir 16 (6) (2000) 2548–2556.
[12] S. Kumar, V.K. Aswal, J. Kohlbrecher, Size-dependent interaction of silica nanoparticles with different surfactants in aqueous solution, Langmuir 28 (25) (2012) 9288–9297.
[13] T. Tran, et al., Study of the synergistic effects between different surfactant types and silica nanoparticles on the stability of liquid foams at elevated temperature, Fuel 315 (2022), 122818.
[14] Y. Wu, et al., Stability mechanism of nitrogen foam in porous media with silica nanoparticles modified by cationic surfactants, Langmuir 34 (27) (2018) 8015–8023.
[15] S. Boakye-Ansah, M.A. Khan, M.F. Haase, Controlling surfactant adsorption on highly charged nanoparticles to stabilize bijels, J. Phys. Chem. C. 124 (23) (2020) 12417–12423.
[16] Z.-G. Cui, et al., Effects of surfactant structure on the phase inversion of emulsions stabilized by mixtures of silica nanoparticles and cationic surfactant, Langmuir 26 (7) (2010) 4717–4724.
[17] R.S. Kumar, et al., Impact of anionic surfactant on stability, viscoelastic moduli, and oil recovery of silica nanofluid in saline environment, J. Pet. Sci. Eng. 195 (2020), 107634.
[18] Z. Liu, et al., Understanding the stability mechanism of silica nanoparticles: the effect of cations and EOR chemicals, Fuel 280 (2020), 118650.
[19] P. Li, M. Ishiguro, Adsorption of anionic surfactant (sodium dodecyl sulfate) on silica, Soil Sci. Plant Nutr. 62 (3) (2016) 223–229.
[20] C. Flood, et al., Effects of surfactants and electrolytes on adsorbed layers and particle stability, Langmuir 24 (14) (2008) 7323–7328.
[21] S. Kumar, V. Aswal, Tuning of nanoparticle–surfactant interactions in aqueous system, J. Phys.: Condens. Matter 23 (3) (2010), 035101.
[22] P. Li, et al., Comparison of same carbon chain length cationic and anionic surfactant adsorption on silica, Colloids Interfaces 4 (3) (2020) 34.
[23] C. Maltesh, P. Somasundaran, Binding of sodium dodecyl sulfate to polyethylene oxide at the silica—water interface, J. Colloid Interface Sci. 153 (1) (1992) 298–301.
[24] G.R. Iglesias, et al., Interactions between large colloids and surfactants, Soft Matter 7 (10) (2011) 4619–4622.
[25] S. Ahualli, et al., Adsorption of anionic and cationic surfactants on anionic colloids: supercharging and destabilization, Langmuir 27 (15) (2011) 9182–9192.
[26] N.R. Biswal, N. Rangera, J.K. Singh, Effect of different surfactants on the interfacial behavior of the n-hexane–water system in the presence of silica nanoparticles, J. Phys. Chem. B 120 (29) (2016) 7265–7274.
[27] H. Ma, M. Luo, L.L. Dai, Influences of surfactant and nanoparticle assembly on effective interfacial tensions, Phys. Chem. Chem. Phys. 10 (16) (2008) 2207–2213.
[28] S. Al-Anssari, et al., Stabilising nanofluids in saline environments, J. Colloid Interface Sci. 508 (2017) 222–229.
[29] K.W. Trzaskus, et al., Fouling behavior of silica nanoparticle-surfactant mixtures during constant flux dead-end ultrafiltration, J. Colloid Interface Sci. 506 (2017) 308–318.
[30] S.S. Khalilinezhad, et al., Mechanistic modeling of nanoparticles-assisted surfactant flood, Arab. J. Sci. Eng. 43 (2018) 6609–6625.
[31] Z. Huang, Z. Yan, T. Gu, Mixed adsorption of cationic and anionic surfactants from aqueous solution on silica gel, Colloids Surf. 36 (3) (1989) 353–358.
[32] Q. Sun, et al., Aqueous foam stabilized by partially hydrophobic nanoparticles in the presence of surfactant, Colloids Surf. A: Physicochem. Eng. Asp. 471 (2015) 54–64.
[33] S. Li, Z. Li, P. Wang, Experimental study of the stabilization of CO_2 foam by sodium dodecyl sulfate and hydrophobic nanoparticles, Ind. Eng. Chem. Res. 55 (5) (2016) 1243–1253.
[34] H. Katepalli, A. Bose, Response of surfactant stabilized oil-in-water emulsions to the addition of particles in an aqueous suspension, Langmuir 30 (43) (2014) 12736–12742.
[35] A. Thibaut, et al., Adsorption of an aqueous mixture of surfactants on silica, Langmuir 16 (24) (2000) 9192–9198.
[36] M. Eftekhari, et al., The influence of negatively charged silica nanoparticles on the surface properties of anionic surfactants: electrostatic repulsion or the effect of ionic strength? Phys. Chem. Chem. Phys. 22 (4) (2020) 2238–2248.
[37] L.S. Wan, P.K. Poon, Effect of salts on the surface/interfacial tension and critical micelle concentration of surfactants, J. Pharm. Sci. 58 (12) (1969) 1562–1567.
[38] K.A. Snyder, et al., Estimating the electrical conductivity of cement paste pore solutions from OH−, K+ and Na+ concentrations, Cem. Concr. Res. 33 (6) (2003) 793–798.
[39] A. Domínguez, et al., Determination of critical micelle concentration of some surfactants by three techniques, J. Chem. Educ. 74 (10) (1997) 1227.
[40] J.W. Swan, E.M. Furst, A simpler expression for Henry's function describing the electrophoretic mobility of spherical colloids, J. Colloid Interface Sci. 388 (1) (2012) 92–94.
[41] S. Shim, et al., Diffusiophoresis in the presence of a pH gradient, Phys. Rev. Fluids 7 (11) (2022), 110513.
[42] S. Bhattacharjee, DLS and zeta potential–what they are and what they are not? J. Control. Release 235 (2016) 337–351.
[43] H. Mateos, et al., Measurement of the zeta-potential of solid surfaces through Laser Doppler Electrophoresis of colloid tracer in a dip-cell: Survey of the effect of ionic

strength, pH, tracer chemical nature and size, Colloids Surf. A: Physicochem. Eng. Asp. 576 (2019) 82–90.
[44] W. Brown, J. Zhao, Adsorption of sodium dodecyl sulfate on polystyrene latex particles using dynamic light scattering and zeta potential measurements, Macromolecules 26 (11) (1993) 2711–2715.
[45] CRC handbook of chemistry and physics. 1977.
[46] M. Sulpizi, M.-P. Gaigeot, M. Sprik, The silica–water interface: how the silanols determine the surface acidity and modulate the water properties, J. Chem. Theory Comput. 8 (3) (2012) 1037–1047.
[47] M. Onizhuk, et al., Dissociation constants of silanol groups of silic acids: quantum chemical estimations, J. Struct. Chem. 59 (2018) 261–271.
[48] M. Pfeiffer-Laplaud, et al., Bimodal acidity at the amorphous silica/water interface, J. Phys. Chem. C. 119 (49) (2015) 27354–27362.
[49] O. Matarredona, et al., Dispersion of single-walled carbon nanotubes in aqueous solutions of the anionic surfactant NaDDBS, J. Phys. Chem. B 107 (48) (2003) 13357–13367.
[50] W.M. de Vos, S. Lindhoud, Overcharging and charge inversion: finding the correct explanation (s), Adv. Colloid Interface Sci. 274 (2019), 102040.
[51] B. Li, E. Ruckenstein, Adsorption of ionic surfactants on charged solid surfaces from aqueous solutions, Langmuir 12 (21) (1996) 5052–5063.
[52] M. Anyfantakis, et al., Modulation of the coffee-ring effect in particle/surfactant mixtures: the importance of particle–interface interactions, Langmuir 31 (14) (2015) 4113–4120.
[53] J. Vinogradov, M.D. Jackson, M. Chamerois, Zeta potential in sandpacks: effect of temperature, electrolyte pH, ionic strength and divalent cations, Colloids Surf. A: Physicochem. Eng. Asp. 553 (2018) 259–271.
[54] T.L. Doane, et al., Nanoparticle ζ-potentials, Acc. Chem. Res. 45 (3) (2012) 317–326.
[55] M. Mullet, et al., Surface electrochemical properties of mixed oxide ceramic membranes: Zeta-potential and surface charge density, J. Membr. Sci. 123 (2) (1997) 255–265.
[56] E. Saka, C. Güler, The effects of electrolyte concentration, ion species and pH on the zeta potential and electrokinetic charge density of montmorillonite, Clay Miner. 41 (4) (2006) 853–861.
[57] J. Liu, et al., Influence of ionic strength on the surface charge and interaction of layered silicate particles, J. Colloid Interface Sci. 432 (2014) 270–277.
[58] A.J. Prosser, E.I. Franses, Adsorption and surface tension of ionic surfactants at the air–water interface: review and evaluation of equilibrium models, Colloids Surf. A: Physicochem. Eng. Asp. 178 (1–3) (2001) 1–40.
[59] R.G. Bates, B.R. Staples, R.A. Robinson, Ionic hydration and single ion activities in unassociated chlorides at high ionic strengths, Anal. Chem. 42 (8) (1970) 867–871.
[60] V. Fainerman, et al., Surface tension isotherms, adsorption dynamics and dilational visco-elasticity of sodium dodecyl sulphate solutions, Colloids Surf. A: Physicochem. Eng. Asp. 354 (1–3) (2010) 8–15.